

# An All-Plastic Field-Effect Nanofluidic Diode Gated by a Conducting Polymer Layer

Gonzalo Pérez-Mitta,\* Waldemar A. Marmisollé, Christina Trautmann, María Eugenia Toimil-Molares, and Omar Azzaroni\*

Dedicated to Professor Roberto Salvarezza on the occasion of his 65th birthday

The design of an all-plastic field-effect nanofluidic diode is proposed, which allows precise nanofluidic operations to be performed. The fabrication process involves the chemical synthesis of a conductive poly(3,4-ethylenedioxythiophene) (PEDOT) layer over a previously fabricated solid-state nanopore. The conducting layer acts as gate electrode by changing its electrochemical state upon the application of different voltages, ultimately changing the surface charge of the nanopore. A PEDOT-based nanopore is able to discriminate the ionic species passing through it in a quantitative and qualitative manner, as PEDOT nanopores display three well-defined voltage-controlled transport regimes: cation-rectifying, non-rectifying, and anion rectifying regimes. This work illustrates the potential and versatility of PEDOT as a key enabler to achieve electrochemically addressable solid-state nanopores. The synergism arising from the combination of highly functional conducting polymers and the remarkable physical characteristics of asymmetric nanopores is believed to offer a promising framework to explore new design concepts in nanofluidic devices.

Currently there is a growing interest in developing nanofluidic devices with the capacity to externally regulate the flow of different molecules within miniaturized integrated circuits. With the rise of nanofluidics starting approximately twenty years ago, large advances in the fabrication of devices that control ionic carriers have been achieved.<sup>[1–4]</sup> Nanofluidic devices may have similar functioning as biological ion channels that behave either as ionic resistor or diode.<sup>[5,6]</sup> Moreover, complex systems such

as field-effect transistors (FET) and bipolar transistors have been fabricated with amazing technological applications in fields such as biosensing or surface science.<sup>[7–11]</sup> For example, a device to sequence DNA strands based on nanopore resistors has recently been put on the market.<sup>[13]</sup> These first advances can be compared to the progress in electron conduction reached by the semiconductor technologies.

However, there is still a long way to achieve complete control over the transport of molecules in integrated ionic circuits. Ionic diodes are very promising because they regulate the selective transport of ions in a voltage dependent manner, i.e., selectivity can be easily detected by ionic current rectification in current–voltage measurements.<sup>[14]</sup> Either cations or anions can be excluded as current carriers depending on the net surface charge of the nanofluidic structure.<sup>[15]</sup>

Several attempts have been made to modulate the response of ionic diodes in a manner that allows changing the magnitude and direction of this rectification at will. Until now, this has been effectively obtained only by specific chemical stimuli in solution, such as the pH.<sup>[16–18]</sup> Aiming at implementing such nanofluidic devices in more complex designs, there is a strong interest in being able to modulate ionic currents by experimental inputs that are easier to control, such as voltage, light, or temperature.<sup>[19]</sup> In this regard, our group has already demonstrated that the combination of solid-state polymer nanopores and electrochemically synthesized conducting polymers is a promising starting platform.<sup>[20]</sup>

Herein, we present the fabrication of a field-effect tunable ionic diode by implementing the chemically synthesized conducting polymer poly(3,4-ethylenedioxythiophene) (PEDOT) upon a solid-state polymeric nanopore. The PEDOT layer enhances the rectification properties of the nanopore and most importantly, acts as a field-effect nonmetallic gate electrode by changing its electrochemical state by applying different voltages. A strong reversion and modulation of the surface charge and consequently the rectification efficiency is observed.

Poly(ethylene terephthalate) (PET) nanochannels were fabricated by means of ion-track etching nanotechnology.<sup>[21]</sup> The technique is based on the irradiation of polymer foils with swift

G. Pérez-Mitta, Dr. W. A. Marmisollé, Prof. O. Azzaroni  
Instituto de Investigaciones Físicoquímicas  
Teóricas y Aplicadas (INIFTA)  
Departamento de Química  
Facultad de Ciencias Exactas  
Universidad Nacional de La Plata  
CONICET – CC 16 Suc. 4, 1900 La Plata, Argentina  
E-mail: gperezmitta@inifta.unlp.edu.ar; azzaroni@inifta.unlp.edu.ar  
Prof. C. Trautmann, Dr. M. E. Toimil-Molares  
GSI Helmholtzzentrum für Schwerionenforschung  
64291 Darmstadt, Germany  
Prof. C. Trautmann  
Technische Universität Darmstadt  
Material-Wissenschaft  
64287 Darmstadt, Germany

DOI: 10.1002/adma.201700972

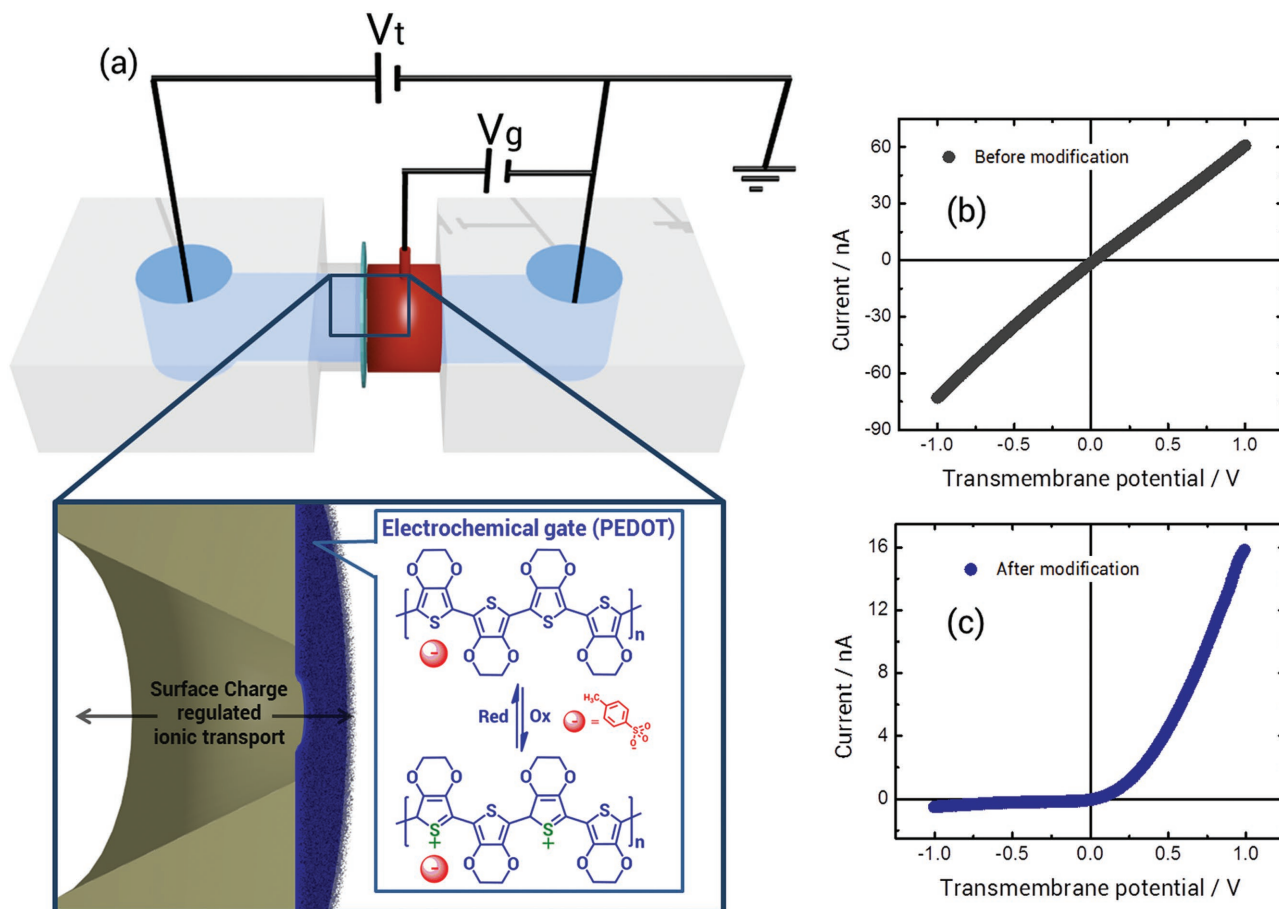


**Figure 1.** a) Scheme of the electrochemical set-up used for the experiments, constituting two hollow cells halves that are connected through a single nanochannel-containing membrane. One of the compartments has attached a solution isolated copper ring that connects electrically with the PEDOT layer acting as gate and allows applying different gate voltages  $V_g$ .  $V_t$  denotes the transmembrane potential applied between the two cell compartments. The enlarged scheme of the membrane shows the PEDOT/tosylate-coated-nanochannel (blue) and its electrochemical conversion when applying a voltage that ultimately produces a change of the  $I$ - $V$  behavior. b,c) Current-voltage curves before (Ohmic) (b) and after (c) PEDOT coating (rectification). The reduction of the ionic conductance in (c) indicates partial closure while the increase of the rectification efficiency indicates the asymmetric modification of the nanochannel.

heavy ions followed by chemical etching of the ion tracks.<sup>[22]</sup> Special etching conditions allow the fabrication of channels with asymmetric conical geometry.<sup>[23]</sup> The surface of a membrane containing one single conical pore was coated by a thin PEDOT layer. Experimental details of the track etching and coating procedure can be found in the experimental section. The PEDOT layer reduces the effective pore cross-section and partially fills the opening region. We thus started our experiments with an initial small opening pore diameter of  $\approx 150$  nm and a large base diameter of  $\approx 1000$  nm. These values are several orders of magnitude higher than the Debye length at salts concentrations between  $10 \times 10^{-3}$ – $100 \times 10^{-3}$  M ( $\approx 1$  nm). As a consequence of this, the depletion of ionic carriers at the tip of the nanochannels, which ultimately produces the current rectification, becomes negligible for large pores and the behavior becomes ohmic. In order to observe ionic rectification in ion track-etched nanochannels fabricated using the surfactant assisted technique (bullet-like geometry), the use of nanochannels with tip diameters smaller than  $\approx 50$ – $70$  nm is necessary.<sup>[22b,23]</sup>

The measurements were performed in an electrochemical cell (Figure 1a and Figure S1, Supporting Information) employing an electrolyte concentration within the physiological range ( $100 \times 10^{-3}$  M KCl). As evidenced by the linearity of the current-voltage curve ( $I$ - $V$ ) the pore showed Ohmic behavior prior to proceeding with the chemical modification (Figure 1b).

The coating with PEDOT was performed selectively on the small opening side of the conical channel by spin-coating using an iron (III) tosylate solution as oxidant and stabilizer.<sup>[25]</sup> After the coating, the  $I$ - $V$  curve shows a remarkable rectification of the ionic current (Figure 1c) presumably caused by increased asymmetry and higher confinement of the electrolyte solution, both caused by reduced channel opening. Ellipsometry measurements showed that a layer of  $\approx 60$  nm was deposited after each cycle of spin-coating and polymerization of PEDOT (Figure S2, Supporting Information). This kind of top-down approach for the synthesis of nanofluidic diodes is very promising for developing devices from non-nanometric architectures.<sup>[26]</sup> In order to characterize the PEDOT films deposited on the PET foils, Raman spectroscopy and contact angle measurements were

performed (Figure S3, Supporting Information). The Raman spectra presented all the features assigned to PEDOT while the wetting data showed a slight increase in the hydrophobicity of the foil after the deposition.

Once the polymeric gate electrode was fabricated, its electrochemical performance was studied by cyclic voltammetry (CV) in  $100 \times 10^{-3}$  M KCl. The electrochemical potential was scanned between  $-2$  and  $2$  V (Figure S3, Supporting Information). Two oxidation peaks ( $0.2$  and  $1.6$  V) and one reduction peak ( $-0.5$  V) were observed, which is in agreement with previously reported electrochemical data of PEDOT.<sup>[27,28]</sup> The oxidation is known to produce a conducting form, due to the emergence of polarons, which are cationic radicals that transport the current as holes (p-type).<sup>[29,30]</sup> Therefore, oxidizing the polymer is sometimes referred as p-doping although it is also known as anion-doping due to the inclusion of anions within the polymer to compensate the positive charges.<sup>[31]</sup> On the other hand, the reduction of the polymer is known as n-doping or cation doping for similar reasons. It is important to mention that for the n-doping, the negative charges stem from counter ions included during the synthesis for electrostatic neutralization, for this experiments the molecule was tosylate.

The type of doping of the PEDOT film becomes essential for nanofluidic applications as it modifies the nature of the counter ions around the channel walls and, concomitantly, the type of carrier shuttling the ionic current through the nanochannel. In this way, the doping level of the polymer determines the type and magnitude of the ionic conductance of the nanochannel. Additionally, this doping level can be easily and reversibly tuned by electrochemical (voltage-driven) reactions, constituting an analogous of the gate electrode in field-effect devices.

We explored this field-effect control over the ionic carriers in the same configuration shown in Figure 1a, by applying different gate voltages ( $V_g$ ) to the polymer film (oxidizing or reducing the PEDOT) and simultaneously recording the  $I$ - $V$  curves by applying a transmembrane voltage ( $V_t$ ) scan (Figure 1). The use of a bipotentiostat allowed the application of different and independent voltage routines for both  $V_g$  and  $V_t$ .

As-synthesized PEDOT is in the conducting oxidized state (p-doped). By electrochemical reduction at  $V_g = -0.2$  V, the  $I$ - $V$

curves become almost linear. The absence of rectification effects indicates that the polymer film is mainly neutral (Figure 2). The application of more negative gate voltages ( $V_g$ ) – below  $-0.2$  V (further electrochemical reduction, n-doping) – induces negative rectification, related to higher cation selectivity. In contrast, oxidation or p-doping of the PEDOT film increases the positive rectification, related to the anion selectivity. For  $V_g$  higher than  $0.8$  V the film starts to degrade due to over-oxidation reactions. The large peak observed in the CV at  $1.6$  V is related to this degradation process (Figure S3, Supporting Information and insets in Figure 2).<sup>[32]</sup>

Rectification factors ( $f_{rec}$ ) were calculated as the quotient of the currents at  $V_t = \pm 1$  V, with the numerator being the larger current value. In order to clearly observe the behavior of  $f_{rec}$  at different gate voltages,  $f_{rec}$  was multiplied by a factor  $-1$  if the larger current was positive. In this way it is possible to qualitatively relate each  $f_{rec}$  to a certain surface charge: negative rectification means a negative surface charge and vice versa. Below the over-oxidation potential,  $f_{rec}$  shows a linear trend on the applied voltage ( $V_g$ ) (Figure 3a), meaning that the concentration of positive species, i.e., polarons, within the PEDOT film grows monotonically with the oxidation of the PEDOT layer. Electron paramagnetic resonance experiments have shown a similar response, with the difference that after  $0.2$  V the concentration of paramagnetic species decreases as they pair forming diamagnetic species.<sup>[33]</sup> Since the  $f_{rec}$  value is related to the net charge on the surface instead of magnetic properties we are able to observe the increment of the concentration of positive centers, a feature never reported before.

The behavior of  $f_{rec}$  with doping charges is also illustrated in Figure 3b showing that changes in the nanochannel selectivity are strongly regulated by the type of doping of the PEDOT film acting as gate electrode. PEDOT gated nanochannels show cation selectivity for n-doping ( $<-0.2$  V) and anion selectivity for the p-doping ( $>0.2$  V). Our approaches thus allow us to transduce a pure electronic input signal into an iontronic output.<sup>[34]</sup> Doping charges were calculated from the integration of the current–time curves at different applied voltages to the gate as explained in the Supporting Information.

For a given  $V_t$ , the application of different gate voltages can directly be transduced into changes in the nanochannel's

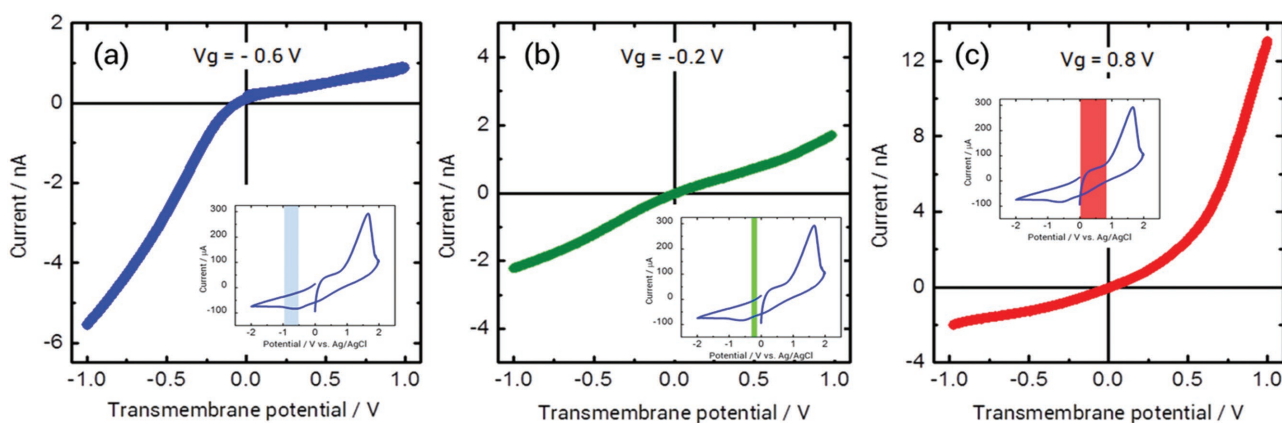


**Figure 2.** Current–voltage curves for a PEDOT-modified nanochannel at three different gate voltages ( $V_g$ ), a)  $-0.6$  V, b)  $-0.2$  V, and c)  $0.8$  V evidencing cation selectivity, neutralization, and anion selectivity, respectively. Insets show regions of the cyclic voltammetry of PEDOT affected by each  $V_g$ .

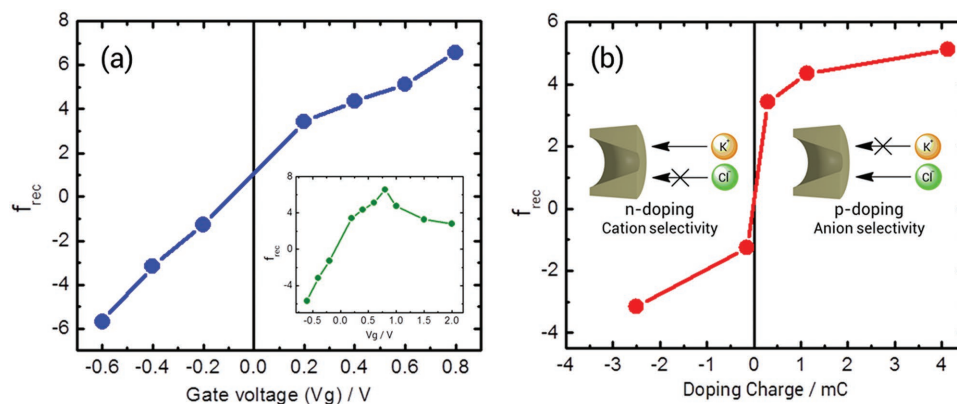


**Figure 3.** a) Rectification factor  $f_{rec}$  versus gate voltage for a PEDOT coated PET nanochannel. The inset shows the complete curve including  $V_g \geq 1$  where the oxidative degradation of the PEDOT layer takes place. b) Rectification factor versus doping charge of the PEDOT layer yielding clear evidence of the correlation between type of doping and rectification behavior.

ionic conductance, resembling a typical FET measurement (Figure 4a).

The ionic conductance of the nanochannel at  $V_t = 1$  V is presented in Figure 4a as a function of the gate voltage  $V_g$  applied to the PEDOT layer. The two regimes of high and low conductance suggest that the gate voltage can be employed as an “on-off” trigger as it is able to enhance or restrict the passage of ions through the nanochannel. Here, it can be observed that

there is no significant difference for the conductance at different negative gate potentials within the off-state ( $-0.2$ ,  $-0.4$ , and  $-0.6$  V). This feature was further corroborated by measuring the ionic currents at  $V_t = 1$  V for different voltages within the off-regime (Figure S5, Supporting Information).

As illustrated in Figure 4b, we observe the “ON-OFF” effect on the ionic current by alternately switching  $V_g$  from on-state ( $V_g = 0.2$  V) to off-state ( $V_g = -0.2$ ) region. Ionic currents

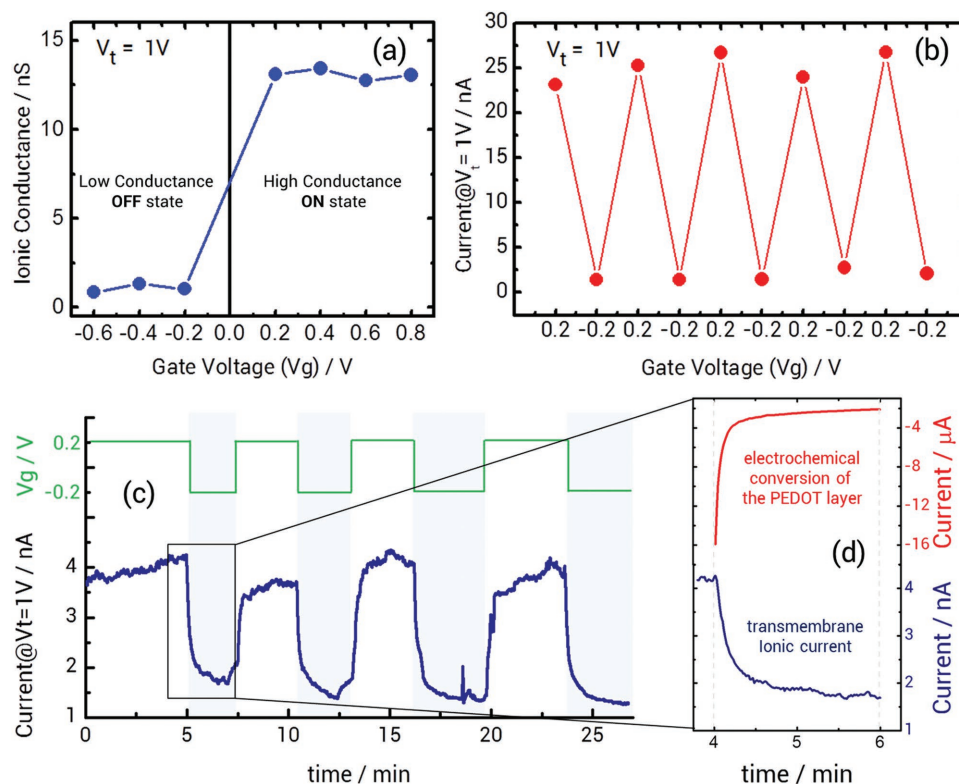


**Figure 4.** a) Ionic conductance of nanochannel versus gate voltage for a fixed transmembrane voltage,  $V_t = 1$ . The plot displays two well-defined conductance states, “ON” and “OFF”. b) Transmembrane ionic current measured at  $V_t = 1$  V and cycled between  $V_g = -0.2$  V (“OFF” state) and  $V_g = 0.2$  V (“ON” state). A good reversibility is observed for repeated cycling. c) Current–time plot for a PEDOT-modified nanochannel showing the reversible gating of the ionic current. d) Chronoamperometric response of the PEDOT film (red) and ionic current–time plot for the nanochannel (blue) measured simultaneously under the same gate voltage ( $-0.2$  V). (a–d) were measured using different sets of nanochannels.

increase between the on and off state by about 2500% as a consequence of the change in the nanochannel conductance. One interesting point that needs to be underlined is that the response of the PEDOT film and its corresponding nanofluidic effect occurs almost immediately after the application of the gate voltage, a feature that can be clearly observed from current–time plots showing the reversible gating of the ionic current upon applying a voltage routine between on- and off-states (Figure 4c). This dynamic behavior of the PEDOT-modified nanochannel is very interesting because it allows a fast switching of the ionic current. A comparison between the chronoamperometry of the PEDOT film at a certain gate voltage (e.g.,  $-0.2$  V) with its corresponding ionic current–time behavior allows observing the coupling between the electrochemistry of the gate film and the control of the ionic transport of the nanofluidic diode (Figure 4d). It is important to point out that the results presented in panels (a), (b), and (c,d) of Figure 4 are highly reproducible and correspond to experiments performed using different nanochannels (Figure S6, Supporting Information).

In conclusion, we have demonstrated the fabrication of a fully tunable field-effect nanofluidic diode by chemically polymerizing the conducting polymer PEDOT and coating it onto the surface of a PET membrane containing a single conical nanochannel. The PEDOT layer behaves as a gate electrode allowing the precise control over both the direction and the magnitude of the rectified ionic current. Combining different transmembrane and gate voltages complete control of the ionic current passing through the nanochannel is evidenced. To our knowledge, this is the first time that an electrochemically gated nanofluidic diode is shown to work under physiological saline conditions; previous works reported systems performing rectification only at concentrations below  $1 \times 10^{-3}$  M.<sup>[19]</sup> Our results reveal that PEDOT is a very promising electrochemically-responsive platform fully compatible with future nanofluidic devices displaying complex functional features, such as those demanded by strategic areas such as sensing or energy conversion.<sup>[35]</sup> It is important to remark that no metallic electrodes were involved neither in the PEDOT synthesis nor in the device fabrication which makes this procedure simple, more biocompatible, and cost-effective. We believe that this proof-of-concept system is a promising prototype for the next generation of integrated nanofluidic circuits.

## Experimental Section

**Materials:** The monomer 3,4-ethylenedioxythiophene (EDOT), iron (III) p-toluenesulfonate hexahydrate, and potassium chloride were purchased from Sigma–Aldrich and used as received.

**Etching Procedure:** PET foils of 12  $\mu\text{m}$  of thickness were irradiated with one individual swift heavy ion (e.g., 2 GeV Au) at GSI Helmholtzzentrum für Schwerionenforschung. The damage induced material along the ion trajectory was removed by selective chemical etching of the irradiated membrane, thus converting the ion track in an open nanochannel. To obtain an asymmetric conical pore shape, the etching procedure was performed in a conductivity cell where one compartment was filled with 6 M NaOH at 60 °C for 7–8 min while the other side contained 6 M NaOH plus a small amount of anionic surfactant Dowfax 2a1 (0.05%). The surfactant is used to protect one face of the membrane from the alkali attack. After the etching the membranes were rinsed several times and stored in deionized water.<sup>[23]</sup>

**PEDOT Synthesis:** To produce PEDOT, the EDOT monomer (24.2  $\mu\text{L}$ ) was dissolved in butanol (440  $\mu\text{L}$ ) along with pyridine (33  $\mu\text{L}$ ) and a 40% solution of iron tosylate in butanol (1.43 ml). The as prepared solution was cleaned with a 0.22  $\mu\text{m}$  filter for organic solutions and spin coated at 1000 rpm (Laurell, model WS-650MZ) on top of the face of the etched PET foil containing the small aperture of the conical channel. The membranes were dried in ambient conditions. The polymerization takes place at this point by oxidation of the monomer promoted by Fe (III) ions. This procedure was repeated 3 times. To remove remaining iron ions, the samples were finally rinsed several times with deionized water.

**Field-Effect Measurements:** A bipotentiostat setup constituted of two Reference 600 potentiostats (Gamry Instruments) was used to independently apply transmembrane and gate voltages and simultaneously measure transmembrane ionic currents. One potentiostat was used to measure the current–voltage curves of the nanochannel using a four electrode configuration whilst the other potentiostat was simultaneously used to apply different gate voltages using a typical three-electrode electrochemical configuration. A detailed picture of the home-made electrochemical cell used for the field-effect measurements is shown in the supporting information (Figure S1, Supporting Information).

## Supporting Information

Supporting Information is available from the Wiley Online Library or from the author.

## Acknowledgements

The authors acknowledge financial support from ANPCyT (PICT 2010–2554, PICT-2013-0905) and from the Deutsche Forschungsgemeinschaft (DFG-FOR 1583). G.P.-M. acknowledges CONICET for a doctoral fellowship. O.A. and W.A.M. are staff members of CONICET. M.E.T and C.T. acknowledge support by the LOEWE project iNAPO funded by the Hessen State Ministry of Higher Education, Research and Arts. The authors thank Esteban Piccinini, Dr. Lorena Cortez and Dr. Catalina von Bidering for technical assistance and helpful discussions.

## Conflict of Interest

The authors declare no conflict of interest.

## Keywords

conducting polymers, ionic rectifiers, nanofluidic devices, PEDOT, solid-state nanopores

Received: February 17, 2017

Revised: March 22, 2017

Published online:

- [1] A. Van den Berg, H. G. Craighead, P. D. Yang, *Chem. Soc. Rev.* **2010**, 39, 899.
- [2] J. H. Han, K. B. Kim, H. C. Kim, T. D. Chung, *Angew. Chem.* **2009**, 48, 3830.
- [3] a) Y. Zhang, K. Kong, L. Gao, Y. Tian, L. Wen, L. Jiang, *Materials* **2015**, 8, 6277; b) H. Zhang, Y. Tian, L. Jiang, *Chem. Commun.* **2013**, 49, 10048; c) J. C. T. Eijkel, A. Van der Berg, *Microfluid. Nanofluid.* **2005**, 1, 249; d) I. Vlassiouk, Z. S. Siwy, *Nano Lett.* **2007**, 7, 552.

- [4] a) Xu Hou, *Adv. Mater.* **2016**, *28*, 7049. b) X. Hou, H. Zhang, L. Jiang, *Angew. Chem.* **2012**, *51*, 5296.
- [5] X. Hou, W. Guo, L. Jiang, *Chem. Soc. Rev.* **2011**, *40*, 2385.
- [6] X. Hou, L. Jiang, *ACS Nano* **2009**, *3*, 3339.
- [7] K. B. Kim, J. H. Han, H. C. Kim, T. D. Chung, *Appl. Phys. Lett.* **2010**, *96*, 143506.
- [8] R. Karnik, K. Castelino, A. Majumdar, *Appl. Phys. Lett.* **2006**, *88*, 123114.
- [9] a) E. B. Kalman, I. Vlasiouk, Z. S. Siwy, *Adv. Mater.* **2008**, *20*, 293; b) Y. Kong, X. Fan, M. H. Zhang, X. Hou, Z. Yue Liu, J. Zhai, L. Jiang, *ACS Appl. Mater. Interfaces.* **2013**, *5*, 7931.
- [10] I. Vlasiouk, T. R. Kozel, Z. S. Siwy, *J. Am. Chem. Soc.* **2009**, *131*, 8211.
- [11] a) E. L. C. J. Blundell, R. Vogel, M. Platt, *Langmuir* **2016**, *32*, 1082; b) A. Sikora, A. G. Shard, C. Minelli, *Langmuir* **2016**, *32*, 2216.
- [12] J. Quick, N. J. Loman, S. Duraffour, J. T. Simpson, E. Severi, L. Cowley, J. A. Bore, R. Koundouno, G. Dudas, A. Mikhail, N. Ouédraogo, B. Afrough, A. Bah, J. H. J. Baum, B. Becker-Ziaja, J. P. Boettcher, M. Cabeza-Cabrerizo, A. Camino-Sánchez, L. L. Carter, J. Doerrbecker, T. Enkirch, I. García-Dorival, N. Hetzelt, J. Hinzmann, T. Holm, L. E. Kafetzopoulo, M. Koropogui, A. Kosgey, E. Kuisma, C. H. Logue, A. Mazzarelli, S. Meisel, M. Mertens, J. Michel, D. Ngabo, K. Nitzsche, E. Pallasch, L. V. Patrono, J. Portmann, J. G. Repits, N. Y. Rickett, A. Sachse, K. Singethan, I. Vitoriano, R. L. Yemanaberhan, E. G. Zekeng, T. Racine, A. Bello, A. A. Sall, O. Faye, O. Faye, N. Magassouba, C. V. Williams, V. Amburgey, L. Winona, E. Davis, J. Gerlach, F. Washington, V. Monteil, M. Jourdain, M. Bererd, A. Camara, H. Somlare, A. Camara, M. Gerard, G. Bado, B. Baillel, D. Delaune, K. Y. Nebie, A. Diarra, Y. Savane, R. B. Pallawo, G. J. Gutierrez, N. Milhano, I. Roger, C. J. Williams, F. Yattara, K. Lewandowski, J. Taylor, P. Rachwal, D. J. Turner, G. Pollakis, J. A. Hiscox, D. A. Matthews, M. K. O'Shea, A. McD. Johnston, D. Wilson, E. Hutley, E. Smit, A. Di Caro, R. Wölfel, K. Stoecker, E. Fleischman, M. Gabriel, S. A. Weller, L. Koivogui, B. Diallo, S. Keïta, A. Rambaut, P. Formenty, S. Günther, M. W. Carroll, *Nature* **2016**, *530*, 228.
- [13] G. Pérez-Mitta, A. G. Albesa, M. E. Toimil-Molares, C. Trautmann, O. Azzaroni, *ChemPhysChem* **2016**, *17*, 1.
- [14] Z. Siwy, E. Heins, C. C. Harrell, P. Kohli, C. R. Martin, *J. Am. Chem. Soc.* **2004**, *126*, 10850.
- [15] a) G. Wang, B. Zhang, J. R. Wayment, J. M. Harris, H. S. White, *J. Am. Chem. Soc.* **2006**, *128*, 7679; b) G. Pérez-Mitta, L. Burr, J. S. Tuninetti, C. Trautmann, M. E. Toimil-Molares, O. Azzaroni, *Nanoscale* **2016**, *8*, 1470.
- [16] H. Zhang, X. Hou, J. Hou, L. Zeng, Y. Tian, L. Li, L. Jiang, *Adv. Funct. Mater.* **2015**, *25*, 1102.
- [17] X. Hou, Y. Liu, H. Dong, F. Yang, L. Li, L. Jiang, *Adv. Mater.* **2010**, *22*, 2440.
- [18] W. Guan, R. Fang, M. A. Reed, *Nat. Commun.* **2011**, *2*, 506.
- [19] G. Pérez-Mitta, W. A. Marmisollé, C. Trautmann, M. E. Toimil-Molares, O. Azzaroni, *J. Am. Chem. Soc.* **2015**, *137*, 15382.
- [20] C. Trautmann, in *Ion Beams in Nanoscience and Technology*, (Eds: R. Hellborg, H. Whitlow, Y. Zhang), Springer-Verlag, Berlin, Germany **2009**, pp. 369–387.
- [21] H. Zhang, X. Hou, Z. Yang, D. Yan, L. Li, Y. Tian, H. Wang, L. Jiang, *Small* **2015**, *11*, 786
- [22] a) G. Pérez-Mitta, A. G. Albesa, W. Knoll, C. Trautmann, M. E. Toimil-Molares, O. Azzaroni, *Nanoscale* **2015**, *7*, 15594. b) P. Y. Apel, I. V. Blonskaya, N. V. Levkovich, O. L. Orelovich, *Pet. Chem.* **2011**, *51*, 555.
- [23] P. Y. Apel, I. V. Blonskaya, S. N. Dmitriev, O. L. Orelovitch, A. Presz, B. A. Sartowska, *Nanotechnology* **2007**, *18*, 305302.
- [24] A. Elschner, S. Kirchmeyer, W. Lövenich, U. Merker, K. Reuter, *PEDOT: Principles and Applications of an Intrinsically Conductive Polymer*, CRC Press, Boca Raton, FL, USA **2011**.
- [25] G. Pérez-Mitta, J. S. Tuninetti, W. Knoll, C. Trautmann, M. E. Toimil-Molares, O. Azzaroni, *J. Am. Chem. Soc.* **2015**, *137*, 6011.
- [26] M. Dietrich, J. Heinze, G. Heywang, F. Jonas, *J. Electroanal. Chem.* **1994**, *369*, 87.
- [27] L. Groenendaal, G. Zotti, P.-H. Aubert, S. M. Waybright, J. R. Reynolds, *Adv. Mater.* **2003**, *15*, 855.
- [28] Y. Harima, T. Eguchi, K. Yamashita, K. Kojima, M. Shiotani, *Synth. Met.* **1999**, *105*, 121.
- [29] Z. W. Sun, A. J. Frank, *J. Chem. Phys.* **1991**, *94*, 4600.
- [30] A.-N. Chowdhijry, Y. Harima, Y. Kunugi, K. Yamashita, *Electrochim. Acta* **1996**, *41*, 1993.
- [31] A. Zykwińska, W. Domagala, B. Pilawa, M. Lapkowska, *Electrochim. Acta* **2005**, *50*, 1625.
- [32] A. Zykwińska, W. Domagala, M. Lapkowski, *Electrochem. Commun.* **2003**, *5*, 603.
- [33] H. Chun, T. D. Chung, *Annu. Rev. Anal. Chem.* **2015**, *8*, 1.
- [34] a) J. A. Arter, D. K. Taggart, T. M. McIntire, R. M. Penner, G. A. Weiss, *Nano. Lett.* **2010**, *10*, 4858; b) Y. Wen, J. Xu, D. Li, M. Liu, F. Kong, H. He, *Synth. Met.* **2012**, *162*, 1308.
- [35] M. Chabinyč, *Nat. Mater.* **2014**, *13*, 119.